

## Direct observation of intramolecular atomic motion in H<sub>2</sub> and D<sub>2</sub> by using electron-atom Compton scattering

Yuichi Tachibana, Masakazu Yamazaki,<sup>\*</sup> and Masahiko Takahashi<sup>†</sup>

*Institute of Multidisciplinary Research for Advanced Materials, Tohoku University, Sendai 980-8577, Japan*



(Received 5 April 2019; published 4 September 2019)

We report electron-atom Compton scattering experiments on the H<sub>2</sub> and D<sub>2</sub> molecules. Energy-loss spectra of electrons quasielastically backscattered at an angle of 135° are measured as a function of azimuthal angle at an incident electron energy of 2.0 keV. Momentum distributions of the H and D atoms due to molecular vibration are extracted from the experimental data by using a protocol that we propose here. The results are successfully compared with theoretical ones predicted by the molecular vibrational wave functions. It is shown that electron-atom Compton scattering has a unique ability to provide direct information about intramolecular motion of each atom with different mass numbers.

DOI: [10.1103/PhysRevA.100.032506](https://doi.org/10.1103/PhysRevA.100.032506)

### I. INTRODUCTION

Atoms in matter are not at rest but are moving at nonzero temperatures. Such atomic motion has long been attracting great attention in a broad range of science and technology areas. For instance, the influence of crystal vibration on x-ray diffraction was first considered in 1914 by Debye [1] and later by Waller [2]. The resulting so-called Debye-Waller factor is now well known as one of the fundamental bases in the studies of x-ray, electron [3], and neutron [4] diffraction by solids. Such is also the case with molecules, for which intramolecular atomic motion has been investigated so far mainly by laser vibrational spectroscopy. Indeed, vibrational spectra provide accurate information about frequencies of normal modes of molecular vibration [5], and they act as the proverbial fingerprint of the structure of a molecule and its structural change [6]. However, such normal modes usually include collective motion of many (or all) of the constituent atoms, and hence the displacement of any of the atoms can be observed only in the form of a linear combination of canonical normal modes [7,8]. Since chemistry is local owing to the short-range nature of chemical forces and an atom sees only its immediate surroundings [9], one may desire to have an experimental technique to observe intramolecular motion of each atom or to decompose the collective-atomic-motion description into the most elementary components.

Recently, an experimental technique called atomic momentum spectroscopy (AMS) was developed by Vos and others [10,11] which employs electron-atom Compton scattering at a large scattering angle ( $\theta > 90^\circ$ ) and at incident electron energies of the order of keV or higher. Here the instantaneous motion of the scattering atom causes Doppler broadening of

the energy of the quasielastically backscattered electrons, with the peak position in the electron-energy-loss spectrum being related to the mass of the scattering atom. Clearly, the use of AMS is a possible way to realize the above-mentioned observation of intramolecular motion of each atom, though each with different mass numbers. Despite the potential ability of AMS, however, there have been no studies toward that end as yet, except the attempt of Vos and others to compare AMS data on such as H<sub>2</sub> [12,13], HD and D<sub>2</sub> [13], H<sub>2</sub>O [14], and CH<sub>4</sub> [15] with a semiclassical model [16] in terms of the sum of contributions of molecular translational, vibrational, and rotational motion. In other words, no AMS studies have been conducted which aim to provide direct information about intramolecular atomic motion. The reason behind this situation is that there is no protocol for excluding contribution of the translational motion of gaseous target molecules from AMS experimental raw data.

In this paper we report AMS experiments on H<sub>2</sub> and D<sub>2</sub>. Momentum distributions due to intramolecular atomic motion are extracted from the experimental raw data by using and testing a protocol that we propose based on our AMS study on the influence of translational motion of rare gas atoms [17]. It is shown that the experimental results are successfully compared with the H and D atomic motion in H<sub>2</sub> and D<sub>2</sub> predicted by the molecular vibrational wave functions. This observation is concrete evidence that AMS can be used as a unique and powerful tool to gain direct information about intramolecular motion of each atom with different mass numbers.

### II. THEORETICAL BACKGROUND

Basically, the AMS scattering process can be described, within the plane-wave impulse approximation (PWIA) [15,18], as a billiard-ball-type collision between the incident electron and the scattering atom. Namely, the scattering target atom is treated as a “single” free particle so that it absorbs all of the momentum transfer  $\mathbf{q}(=\mathbf{p}_0-\mathbf{p}_1)$  with  $\mathbf{p}_j$ 's ( $j=0,1$ ) being the momenta of the incident and

<sup>\*</sup>Present address: Department of Chemistry, Tokyo Institute of Technology, Tokyo 152-8550, Japan.

<sup>†</sup>Author to whom correspondence should be addressed: [masahiko@tohoku.ac.jp](mailto:masahiko@tohoku.ac.jp)

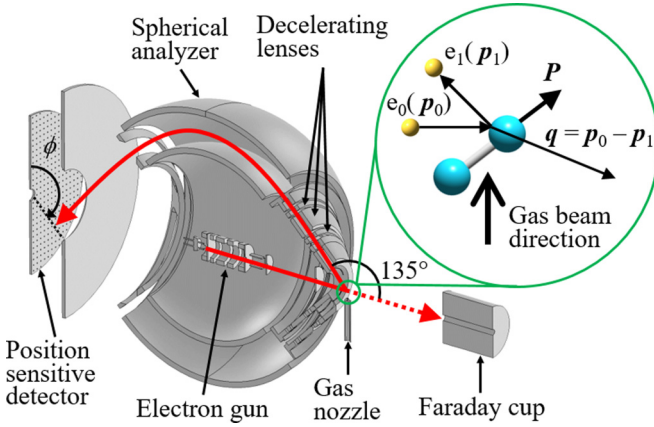


FIG. 1. Schematic of an AMS spectrometer [19] used in the present work.

quasielastically backscattered electrons. The target atom with mass  $M$  and momentum  $\mathbf{P}$  thus acquires a recoil energy  $E_{\text{recoil}}$ , through the collision, which is given by

$$E_{\text{recoil}} = \frac{(\mathbf{P} + \mathbf{q})^2}{2M} - \frac{P^2}{2M} = \frac{q^2}{2M} + \frac{\mathbf{P} \cdot \mathbf{q}}{M}. \quad (1)$$

Here the first term in the right-hand side of Eq. (1) is the mean recoil energy  $\bar{E}_{\text{recoil}}$  that represents the recoil for scattering from a stationary atom. The second term is the Doppler broadening due to the motion of the target atom before collision. Since the incident electron must lose the energy equal to  $E_{\text{recoil}}$  through the collision to satisfy the law of energy conservation, energy analysis of the scattered electrons can provide direct information about  $\mathbf{P}$  of the initial target atom as its projection onto  $\mathbf{q}$ .

### III. EXPERIMENT

The experiments on  $\text{H}_2$  and  $\text{D}_2$  were performed at an incident electron energy of 2.0 keV by using our AMS apparatus. Details of the apparatus are described elsewhere [19], so only a brief account of it is given here with Fig. 1. An incident electron beam was generated by a thermal electron gun that incorporated a tungsten filament. A typical current of a few hundred nanoamperes was collected in a Faraday cup. Quasielastic electron backscattering occurred where the incident electron beam collided with a gaseous  $\text{H}_2$  or  $\text{D}_2$  molecule in an effusive beam from a gas nozzle. Here high-purity  $\text{H}_2$  (>99.99999%) and  $\text{D}_2$  (>99.6%) gases were obtained from Taiyo Nippon Sanso Corporation and used at room temperature. The scattered electrons were angle-limited by apertures so that a spherical electron energy analyzer accepted those at a scattering angle of  $\theta = 135^\circ \pm 0.4^\circ$  ( $q = 22.4$  a.u.) over azimuthal angle  $\phi$  ranging from  $0^\circ$  to  $72.5^\circ$ , from  $107.5^\circ$  to  $252.5^\circ$ , and from  $287.5^\circ$  to  $360^\circ$ . Decelerating electrostatic lenses were used for the electrons before entrance to the analyzer in order to achieve a higher energy resolution, with a deceleration ratio of around 20:1. The electrons passing through the analyzer were eventually detected with a position-sensitive detector (HEX120o, RoentDek) [20]. The resulting instrumental energy resolution was 0.6 eV FWHM. An

additional AMS measurement was also conducted for Xe in order to partly calibrate the energy scale of the experimental data on  $\text{H}_2$  and  $\text{D}_2$  at each  $\phi$ , under an assumption that  $E_{\text{recoil}}$  of such a heavy atom can be regarded as zero. This assumption is justified by Eq. (1), which predicts  $\bar{E}_{\text{recoil}}$  of Xe to be 0.03 eV, the value being negligibly small compared to the energy resolution of 0.6 eV.

The protocol that we propose to extract information about intramolecular atomic motion from AMS experimental raw data is composed of three procedures. The first is to consider influence of translational motion of a gaseous target molecule to the AMS experimental data. The second is to create an AMS spectrum that is free from the difference in influence of the translational motion. The last is to obtain momentum distribution due to intramolecular atomic motion by a deconvolution procedure. Here we test the validity of the protocol with the experimental data on  $\text{H}_2$  and  $\text{D}_2$  in the following manner.

### IV. RESULTS AND DISCUSSION

Figure 2(a) compares electron-energy-loss spectra of  $\text{H}_2$  with those of  $\text{D}_2$ , measured at the forward ( $\phi = 0^\circ$ ) and backward ( $180^\circ$ ) geometries with respect to the effusive beam direction. It can be seen first that both the  $\text{H}_2$  and  $\text{D}_2$  bands appear at around the expected  $\bar{E}_{\text{recoil}}$  values of 3.7 and 1.9 eV, respectively, and they are energetically separated from each other, showing the ability of AMS to resolve atoms with different mass numbers. Secondly, it can also be seen that forward-backward asymmetry is present in both  $\text{H}_2$  and  $\text{D}_2$ ; their band peak positions at the  $\phi = 0^\circ$  and  $180^\circ$  geometries are different from each other. This is due to effects of translational motion of a gaseous target, as observed and analyzed for He, Ne, Ar, and Kr atoms [17]. Indeed, one can see from Fig. 2(b) that the  $\phi$ -angle dependence of the  $\text{H}_2$  and  $\text{D}_2$  band peak positions are reproduced, as well as the reported one of He with mass similar to those of  $\text{H}_2$  and  $\text{D}_2$  [17], by associated theoretical curves that have been calculated according to our gas beam model using their most probable velocities  $v_{\text{mp}} = \sqrt{3kT/m}$ , with  $k$ ,  $T$ , and  $m$  being the Boltzmann constant, temperature, and mass of the target atom or molecule [17].

Figures 3(a) and 3(b) show  $\phi$ -angle integrated spectra of  $\text{H}_2$  and  $\text{D}_2$ , respectively, which were created by shifting the band peak positions of the electron-energy-loss spectra at each  $\phi$  to the origin of the energy axis, followed by summing up those for each target molecule. Such a summed-up, energy-aligned spectrum of a target atom or molecule is referred to as the AMS spectrum hereafter. Also included in Figs. 3(a) and 3(b) is an AMS spectrum of Xe. Clearly, both the  $\text{H}_2$  and  $\text{D}_2$  AMS spectra are broader than the Xe one, and the degree of the broadness is noticeably larger for the former than for the latter. Since what can cause the Doppler broadening to the  $\text{H}_2$  and  $\text{D}_2$  AMS spectral profiles are molecular vibrational, rotational, and translational motion, the observed difference in broadness must have its source in the three types of molecular movement. We rule out first a possibility of the translational motion, as the AMS spectra of rare gas atoms (He, Ne, Ar, Kr and Xe) having their own different most probable velocities

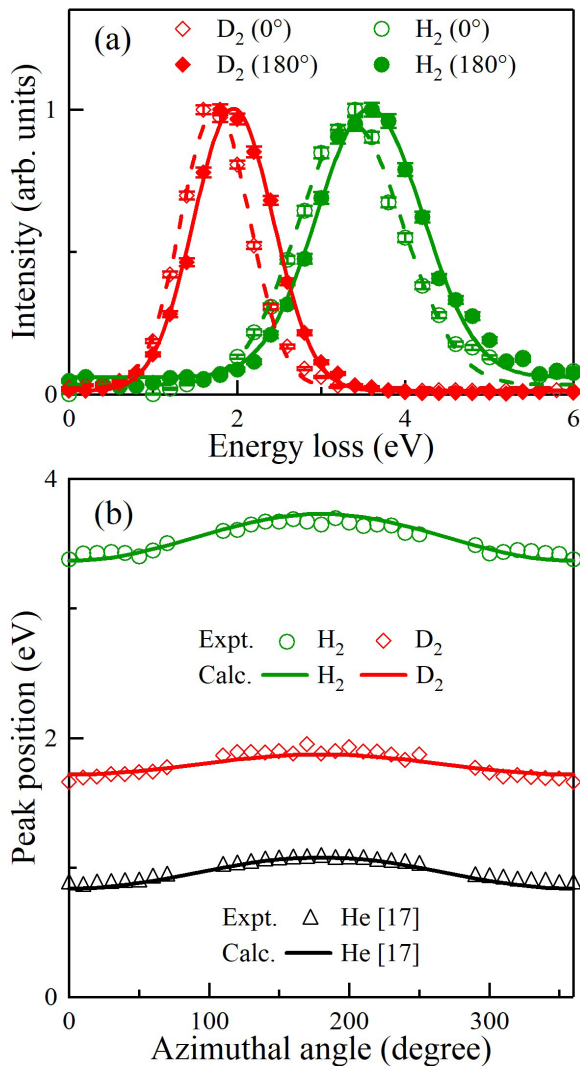


FIG. 2. (a) Comparison of electron-energy-loss spectra of  $\text{H}_2$  and  $\text{D}_2$ , measured at  $\phi = 0^\circ$  and  $180^\circ$ . (b) Variation of experimental and theoretical band peak positions of  $\text{H}_2$  and  $\text{D}_2$  vs  $\phi$ . The He data [17] are presented as a reference.

$v_{\text{mp}}$  at room temperature have been found to be indistinguishable from each other within the instrumental energy resolution [17]. This indicates that AMS spectra in Fig. 3 may be free from the influence of the translational motion, or even if there still remain unknown influence, the  $\text{H}_2$ ,  $\text{D}_2$ , and Xe AMS spectra are affected in the same way. One can therefore remove thoroughly the influence of the translational motion from the  $\text{H}_2$  and  $\text{D}_2$  AMS spectra by recognizing the Xe AMS spectrum as the instrumental response function in a deconvolution procedure.

The vibrational and rotational motion thus remain as a possible source of the difference in broadness observed in Fig. 3. It should be noted, however, that vibrational energy is usually much larger than rotational energy, and hence the kinetic energy fraction of the former is also expected to be much larger than that of the latter. In fact, a semiclassical model calculation [16] indicates that the kinetic energies of the H (D) atom in  $\text{H}_2$  ( $\text{D}_2$ ) due to vibrational and rotational motion at room temperature are 0.068 (0.048) eV and 0.013

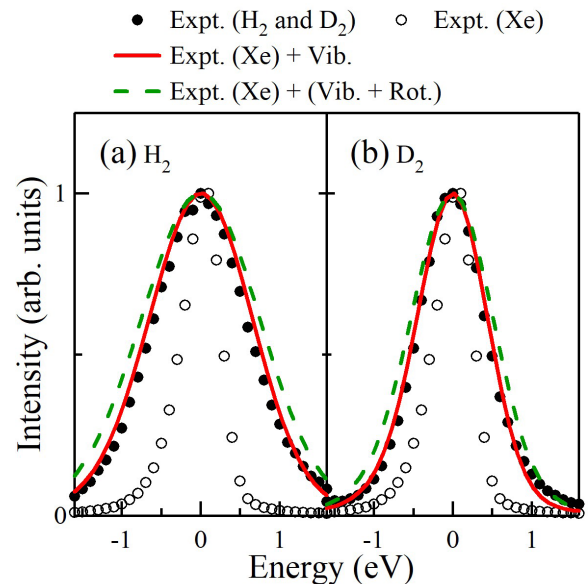


FIG. 3. AMS spectra of (a)  $\text{H}_2$  and (b)  $\text{D}_2$  compared with that of Xe. The solid and dashed lines represent associated theoretical spectra, generated by using the contribution of vibrational motion of a semiclassical model [16] and those of vibrational and rotational motion respectively.

(0.013) eV, respectively. Associated theoretical spectra have then been generated by folding the instrumental response function (the Xe AMS spectrum) with the semiclassical model predictions while assuming Gaussian-like distributions in the AMS spectra [21], and they are also depicted in Fig. 3. It can be seen that the theoretical spectra reproduce the experiments qualitatively, and contribution of molecular vibration almost entirely dominates over that of rotational motion. Based on this observation, we neglect the small contribution of rotational motion and extract information about intramolecular atomic motion from the molecular AMS spectra by a deconvolution procedure.

In general, deconvolution procedures have widely been used to resolve subbands buried in various kinds of spectra [22]. A trial function to be used in the present work has been chosen as follows. First,  $\text{H}_2$  and  $\text{D}_2$  are a diatomic molecule and have only one normal mode of vibration, so the intramolecular motion or momentum distribution of the H(D) atom in  $\text{H}_2$  ( $\text{D}_2$ ) is described by the absolute square of the molecular vibrational wave function in momentum space  $|\Psi(P)|^2$  and is given, within the harmonic oscillator model, by

$$|\Psi(P)|^2 \propto \exp\left(-\frac{P^2}{\mu\hbar\omega}\right), \quad (2)$$

where  $\mu$ ,  $\hbar$ , and  $\omega$  are the reduced mass, the reduced Planck constant, and the angular frequency of the oscillator, respectively. Second, we consider random orientation of the target  $\text{H}_2$  ( $\text{D}_2$ ) molecules with respect to  $\mathbf{q}$ , and the resulting spherically averaged atomic momentum distribution  $I_{\text{vib}}(P)$

has the following form [12,23]:

$$I_{\text{vib}}(P) \propto \int_0^{\pi/2} (1 - \cos 2\Theta) \exp\left(-\frac{P^2}{\mu \hbar \omega \cos^2 \Theta}\right) d\Theta, \quad (3)$$

with  $\Theta$  being the angle between  $\mathbf{q}$  and the molecular axis direction. Furthermore, since the predicted distribution [Eq. (3)] has a cusplike feature at  $P = 0$  as pointed out by Vos [12], we choose the following function  $f(P)$  as a trial function:

$$f(P) = A_1 \exp\left(-\frac{|P|}{W}\right) + A_2 \frac{|P|}{2W} \exp\left(-\frac{|P|}{2W}\right), \quad (4)$$

with  $A_1$ ,  $A_2$ , and  $W$  being fitting parameters. Note that use of the deconvolution procedure with such a trial function is justified only in the case of diatomic molecules, because one knows the answer beforehand; the atomic momentum distribution is predicted simply by the vibrational wave function of the canonical normal mode. However, the same is not true with cases of polyatomic molecules, for which one may develop and apply a new procedure for extracting information about intramolecular atomic motions by using the convolution theorem that the Fourier transform of the convolution is the product of the individual Fourier transforms [24].

Results of the fitting to the  $\text{H}_2$  and  $\text{D}_2$  AMS spectra by the trial function, folded with the instrumental response function, are shown in Figs. 4(a) and 4(b), respectively. It can be seen that the fits reproduce well the experimental data. Nevertheless, one may notice a small bilateral asymmetry of the experimental spectral patterns. It indicates that PWIA is not fully satisfied under the experimental conditions employed, as PWIA should provide symmetric momentum distribution for the randomly oriented molecules [see Eq. (1)]. A similar observation has been made by the AMS study of Vos [12], in which it is discussed that since the leading dominant correction term is odd with respect to  $P$  [18], the term can be cancelled by taking the average of the original spectrum and the right and left inverted one. However, the small differences between the experiments and the fitting curves do not affect the argument of the present paper, so we employ the original spectra in the parameter fitting.

Next, the trial functions with the fitted parameters or the experimentally obtained momentum distributions due to intramolecular atomic motion are plotted by solid lines in Figs. 4(c) and 4(d). Also included in these figures are quantum chemistry predictions calculated by using Eq. (3), and they are shown by dashed lines. Here the vibrational frequencies of 4401 and 3115  $\text{cm}^{-1}$  are taken from the literature for  $\text{H}_2$  and  $\text{D}_2$ , respectively [25]. Good agreement between the experiments and theory are immediately evident. This observation means, on one hand, that the vibrational wave functions of  $\text{H}_2$  and  $\text{D}_2$  are experimentally visualized in momentum space. On the other hand, it means that the momentum distribution of the H (D) atom in  $\text{H}_2$  ( $\text{D}_2$ ) is successfully extracted from the AMS experimental raw data by our proposed protocol. In this regard, it should be stressed that the present work with  $\text{H}_2$  and  $\text{D}_2$  is the most stringent test of the protocol. This is because in an  $N$ -atom system,  $3N - 6$  ( $3N - 5$ ) degrees of freedom are spent with molecular vibration and 3 (2) degrees of freedom are done with molecular rotation; therefore, contribution of vibrational motion to a molecular AMS spectrum becomes

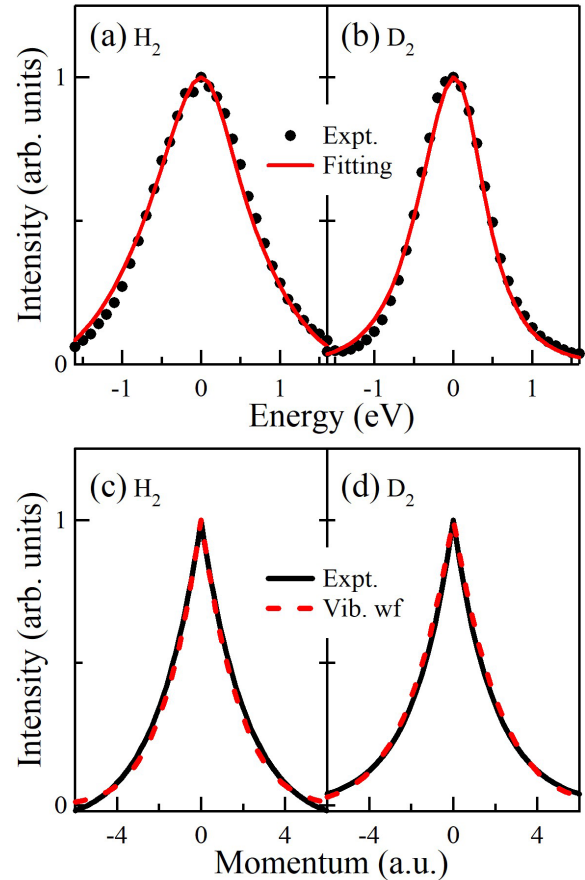


FIG. 4. Figures (a) and (b) show results of fitting to  $\text{H}_2$  and  $\text{D}_2$  AMS spectra, respectively. Figures (c) and (d) represent experimentally obtained momentum distributions due to intramolecular motion of the H atom in  $\text{H}_2$  and the D atom in  $\text{D}_2$ , respectively. The dashed lines are associated distributions calculated by using the molecular vibrational wave functions.

more and more dominant with the increase in  $N$  while that of rotational motion becomes less and less.

## V. SUMMARY

In summary, the present work has reported the AMS experiments on  $\text{H}_2$  and  $\text{D}_2$ . The validity of our suggested protocol has been tested and demonstrated through the comparisons with a momentum-space representation of the molecular vibrational wave functions, opening the door to measurements of intramolecular atomic motion. However, there is an ample room for improvements both theoretically and experimentally. In the theoretical side, to extend the present AMS approach to polyatomic molecules, development of a quantum chemical framework to predict intramolecular motion of a specific constituent atom is required; the use of the vibrational wave function of a canonical normal mode is possible only for the case of diatomic molecules. Moreover, exhaustive treatment for the rotational contribution by quantum chemical calculations also would be a future task of AMS. In the experimental side, improvement of the energy resolution is desired to increase the mass resolution of the scattering atom. In this regard, it should be noted that the present AMS approach is totally different

from the well-known canonical normal mode approach. For instance, AMS is very sensitive to the immediate surroundings of a specific atom, while it cannot discriminate the symmetric stretch mode from the antisymmetric mode; AMS has its merits and demerits, as well as does the canonical normal mode approach. The relationship between the two approaches may be well compared to that between the local molecular orbital and the well-known canonical molecular orbital.

## ACKNOWLEDGMENTS

This work was partially supported by JSPS KAKENHI Grants No. JP25248002, No. JP15K13615, No. JP15H03762, and No. JP17K19095. It was also supported in part by the Management Expenses Grants for National Universities Corporation, the Yamada Science Foundation, and the “Five-Star Alliance” in the “NJRC Materials & Development” research program.

- 
- [1] P. Debye, *Ann. Physik* **348**, 49 (1913).  
[2] I. Waller, *Z. Physik* **17**, 398 (1923).  
[3] J. B. Pendry, *Low-Energy Electron Diffraction* (Academic Press, London, 1974).  
[4] S. W. Lovesey, *Theory of Neutron Scattering from Condensed Matter I, II* (Oxford University Press, Oxford, 1984).  
[5] E. B. Wilson, Jr., J. C. Decius, and P. C. Cross, *Molecular Vibrations: The Theory of Infrared and Raman Vibrational Spectra* (Dover Publications, New York, 1980).  
[6] E. T. J. Nibbering, H. Fidder, and E. Pines, *Annu. Rev. Phys. Chem.* **56**, 337 (2005).  
[7] X. Cheng and R. P. Steele, *J. Chem. Phys.* **141**, 104105 (2014).  
[8] R. C. Couto, V. V. Cruz, E. Ertan, S. Eckert, M. Fondell, M. Dantz, B. Kennedy, T. Schmitt, A. Pietzsch, F. F. Guimarães, H. Ågren, F. Gel'mukhanov, M. Odellius, V. Kimberg, and A. Föhlisch, *Nat. Commun.* **8**, 14165 (2017).  
[9] R. D. Levine, *Molecular Reaction Dynamics* (Cambridge University Press, Cambridge, 2005).  
[10] M. Vos, *Phys. Rev. A* **65**, 012703 (2001).  
[11] M. Vos, G. Cooper, and C. A. Chatzidimitriou-Dreismann, in *Institute of Physics Conference Series*, edited by B. Piraux (Institute of Physics Publishing, Bristol, 2005) Vol. 183, p. 81.  
[12] M. Voss, *J. Phys. B: At. Mol. Opt. Phys.* **49**, 145202 (2016).  
[13] M. Voss and M. R. Went, *J. Phys. B: At. Mol. Opt. Phys.* **42**, 065204 (2009).  
[14] M. Vos, E. Weigold, and R. Moreh, *J. Chem. Phys.* **138**, 044307 (2013).  
[15] M. Vos, *J. Chem. Phys.* **132**, 074306 (2010).  
[16] R. Moreh and D. Nemirovsky, *J. Chem. Phys.* **133**, 084506 (2010).  
[17] M. Yamazaki, Y. Tachibana, and M. Takahashi, *J. Phys. B: At. Mol. Opt. Phys.* **52**, 65205 (2019).  
[18] V. F. Sears, *Phys. Rev. B* **30**, 44 (1984).  
[19] M. Yamazaki, M. Hosono, Y. Tang, and M. Takahashi, *Rev. Sci. Instrum.* **88**, 063103 (2017).  
[20] See <http://www.roentdek.com/> for information about the detector.  
[21] M. P. Paoli and R. S. Holt, *J. Phys. C: Solid State Phys.* **21**, 3633 (1988).  
[22] *Deconvolution of Images and Spectra*, 2nd ed., edited by P. A. Jansson (Academic Press, New York, 1996).  
[23] E. B. Karlsson, *Nucl. Instrum. Methods Phys. Res., Sect. A* **694**, 286 (2012).  
[24] W. H. Press, S. A. Teukolsky, W. T. Vetterling, and B. P. Flannery, *Numerical Recipes in C: The Art of Scientific Computing*, 2nd ed. (Cambridge University Press, New York, 1992).  
[25] K. P. Huber and G. Herzberg, *Molecular Spectra and Molecular Structure* (Van Nostrand Reinhold, New York, 1979), Vol. 4.